

Magic Gold Nanotubes

R. Tuğrul SENGER, Sefa DAĞ, Salim ÇIRACI

Department of Physics, Bilkent University, 06800 Bilkent, Ankara-TURKEY

Received 11.10.2005

Abstract

In recent ultra-high-vacuum transmission-electron-microscopy experiments evidence is found for the formation of suspended gold single-wall nanotubes (SWNTs) composed of five helical strands. Similar to carbon nanotubes, the (n,m) notation defines the structure of the gold SWNTs. Experimentally, only the $(5,3)$ tube has been observed to form among several other possible alternatives. Using first-principles calculations we demonstrate that gold atoms can form both freestanding and tip-suspended, chiral, single-wall nanotubes. Although freestanding, infinite $(5,5)$ tube is found to be energetically the most favorable, the experimentally observed $(5,3)$ tube, suspended between two tips, corresponds to a local minimum in the variation of string-tension with the radius of the structure, which explains the experimental finding. Similarly, we predict the $(4,3)$ tube as a favorable structure yet to be observed experimentally. Analysis of band structure, charge density, and quantum ballistic conductance suggests that the current on these nanowires is less chiral than expected, and there is no direct correlation between the numbers of conduction channels and helical strands.

Key Words: Gold Nanotube, Quantum Conductance

1. Introduction

Ultra thin wires with nanometer-scale thicknesses have interesting mechanical and electronic properties. The studies on nanowires are motivated by the continuing trend of size reduction in electronics from micro to nano scales. Nanowires have potential applications as future nanodevices or as connectors between them. Properties of very thin metal wires are actively studied both experimentally and theoretically [1, 2, 3, 4, 5, 6, 7, 8, 9, 10]; their formation in the form of coaxial shells having helical structures, as well as single atomic chains hanging between two electrodes have been predicted for Cu [5], Al and Pb [6], and Au [7]. Synthesis of single Au atom chain suspended between two Au electrodes has been a real breakthrough in nanotechnology [11, 12]. Furthermore, in UHV-TEM experiments it has been shown that Au nanobridges can transform into several nanometers long suspended chiral nanowires. Interestingly, in agreement with previous theoretical studies, these thin nanowires have the form of helical multiwall structures of specific “magic” sizes [8].

In recent UHV-TEM experiments evidence is found for the formation of Pt and Au single-wall nanotubes (SWNT): For Pt, the tubes consist of 5 or 6 atomic rows that coil helically around the axis of the tube [13]. In the case of gold, the SWNT was observed to be composed of 5 helical strands [10]. The shell of those SWNTs can be constructed from rolling of a triangular network of gold atoms onto a cylinder of radius R as described in Figure 1.

Similar to carbon nanotubes, the (n, m) notation defines the structure of the tube. According to the work by Oshima *et al.* [10] the $(5, 3)$ SWNT (without a linear strand at the center) was a long-lived metastable structure that has been observed between $(7, 3)$ wire (with a strand at the center) and single Au atomic chain synthesized during electron beam thinning of Au thin foil. Apart from being the first observation of a Au chiral SWNT, this interesting result has posed several important questions as to why only $(5, 3)$ tube is observed among tubes with $n = 5$; what other tubes with $n < 5$ are metastable. While the $(5, 3)$ Au tube

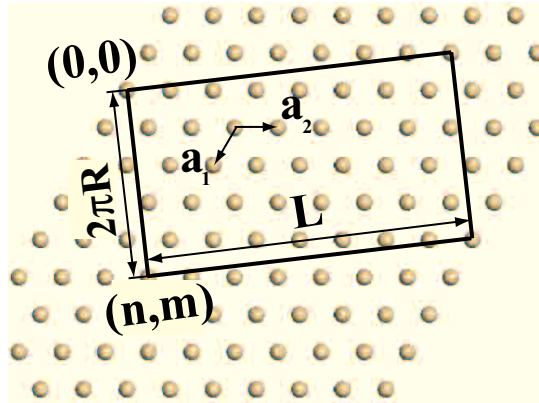


Figure 1. Atomic structure of gold nanotubes are obtained by cylindrical folding of the 2D triangular lattice. Basis vectors of the 2D lattice are \mathbf{a}_1 and \mathbf{a}_2 ; the chiral vector $\mathbf{C} = n\mathbf{a}_1 + m\mathbf{a}_2$, such that the tube circumference is $|\mathbf{C}|$, and radius $R = (n^2 + m^2 - nm)^{1/2}|\mathbf{a}_1|/2\pi$. An (n, m) tube has n helical strands and m defines the chirality. The rectangular area shown in the figure constitutes the unit cell of a $(5,3)$ gold nanotube.

being attached to electrodes is metastable, can free-standing Au SWNTs be stable in the absence of central linear strand? How does the chirality of helical strands influence the ballistic transport? So far neither these questions have been addressed, nor the existence of gold SWNTs has been theoretically demonstrated.

2. Gold Nanotubes

In this study, we show that tubular structures of gold can indeed exist and display interesting electronic and transport properties. Moreover, we explain why only a specific SWNT suspended between two gold tips has been observed experimentally. As single-wall tubular structures of gold, we considered all possible cases with $n = 5, 4, 3$ and $n \geq m > n/2$, since $(n, n-m)$ tubes are equivalent to (n, m) with opposite chirality, and tubes with $n \geq 6$ have large enough radii to accommodate an extra linear strand of gold atoms, therefore lacking a tubular character. In particular, $(4, 2)$ structure also has a non-tubular form corresponding to a dumbbell chain and is not included in our considerations. The structure of $(5, 3)$ tube deduced experimentally has a period approximately five times larger than the lattice parameter of the ideal tube rolled from the undeformed gold sheet [10]. The periodicity length L of the chiral tubes can be altered by a small axial shear. This is achieved by applying a shear strain of $\epsilon \parallel \mathbf{a}_2$ in the triangular network. We take $\epsilon = 0$ to achieve the periodicity of the $(5, 3)$ tube through $2\pi/5$ rotation of helical strands and hence to reduce the number of atoms in the supercell from 190 to 38. Omitting such a small strain ($\epsilon = 0.005$ for $(5, 3)$ tube [10]) does not affect our conclusions, but cuts down computational effort dramatically. We carried out total energy and electronic structure calculations on seven different tubular structures shown in Figure 2, using first-principles pseudopotential plane-wave method [14] within generalized gradient approximation (GGA). All the atomic positions and lattice parameters of tubular structures have been optimized through lowering total energy, atomic forces, and stress. The stability of relaxed structures are tested also by *ab-initio* molecular dynamic calculations carried out at $T = 800$ K. Spin-relaxed calculations yielded zero total magnetic moments for the structures in Figure 2. The analysis of quantum ballistic conductance has been performed by using an *ab-initio* transport software based on localized basis sets and non-equilibrium Green's function formalism [15]. The structural properties of the optimized gold SWNTs are summarized in Table.

The binding (or cohesive) energy $E_b(n, m) = E_T(A) - E_T(n, m)/N$, is calculated as the difference between the energy of single Au atom, $E_T(A)$, and the total energy (per atom) of the fully relaxed (n, m) tubular form having N atoms in the unit cell, $E_T(n, m)/N$. Accordingly, $E_b > 0$ (exothermic) indicates a stable structure corresponding to a local minimum on the Born-Oppenheimer surface. The curvature energy is the energy required to form a tubular form by folding the 2D triangular network, and is expressed as $E_c(n, m) = E_b(2D) - E_b(n, m)$, in terms of the difference of the binding energies in the closed-packed (111)

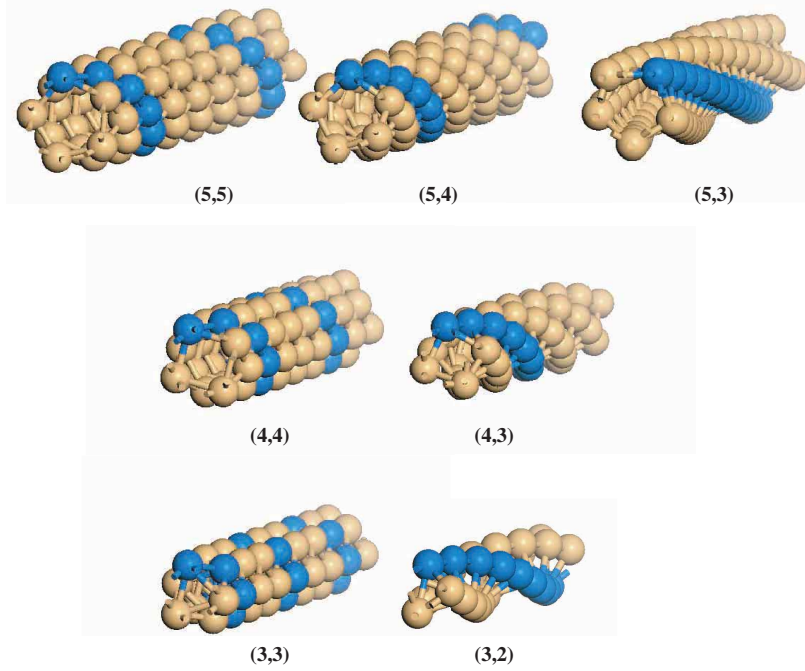


Figure 2. Tubular structures of gold considered in this work. A dark helical strand of atoms highlights the chirality of the tubes. The radius R and period L are modified upon relaxation of the tubular structure.

atomic plane, and in the (n, m) tube. For the relaxed 2D triangular network we found $E_b(2D) = 2.84$ eV/atom. As expected, $E_c(n, m)$ increases with decreasing R . The calculated curvature energies comply with the expression obtained from classical elasticity theory $E_c = Yw^3\Omega/24R^2$ (Y : Young's modulus, w : thickness of the tube, Ω : atomic volume), and are fitted to an expression $E_c = \alpha/R^2$ in Figure 3.

Table. Structural properties and energetics of relaxed chiral gold nanotubes (n, m) . There are N atoms in one unit cell which has length L and radius R , both expressed in Å units. E_b and E_c are the binding and curvature energies per atom in units of eV, respectively. The string tension of the tip-suspended tube, f , has units eV/Å.

Structure	N	L	R	E_b	E_c	f
(5,5)	10	4.63	2.44	2.66	0.18	1.188
(5,4)	14	7.15	2.24	2.60	0.24	1.179
(5,3)	38	20.73	2.12	2.58	0.26	1.154
(4,4)	8	4.60	2.04	2.54	0.30	1.166
(4,3)	26	16.91	1.85	2.52	0.32	1.062
(3,3)	6	4.39	1.71	2.41	0.43	1.083
(3,2)	14	12.28	1.51	2.31	0.53	1.017

All the gold nanotubes given in Table are stable when they are standing free. The cohesive energy values, E_b , given in Table gradually decreases with decreasing R . The distribution of calculated Au-Au bond lengths in the relaxed (5,5) tube has a sharp peak at $d = 2.76\text{Å}$, and relatively weaker individual peaks in the range of $2.85 < d < 2.89\text{Å}$. This distribution is, however, modified in the (5,4) and (5,3) tubes, where the sharp peak at $d = 2.76\text{Å}$ tends to weaken and distribute in a wider range. The shortest d 's correspond to the bonds forming the helical strands. As far as applications as interconnect or nanodevice are concerned, it is important to know whether the free-standing but finite length gold SWNTs are stable. The structure optimization of free $4L$ long (5,5) SWNT with open ends has resulted in a stable structure with negligible rearrangements of atoms relative to the infinite tube. Most importantly, the open ends have not been capped. The stability of gold SWNTs against clustering is somewhat nontrivial, though not

totally unexpected. Noting that free-standing finite zigzag chains of gold are found to be stable [16], the present tubular structures are expected to be even more resistant to clustering owing to their higher atomic coordination.

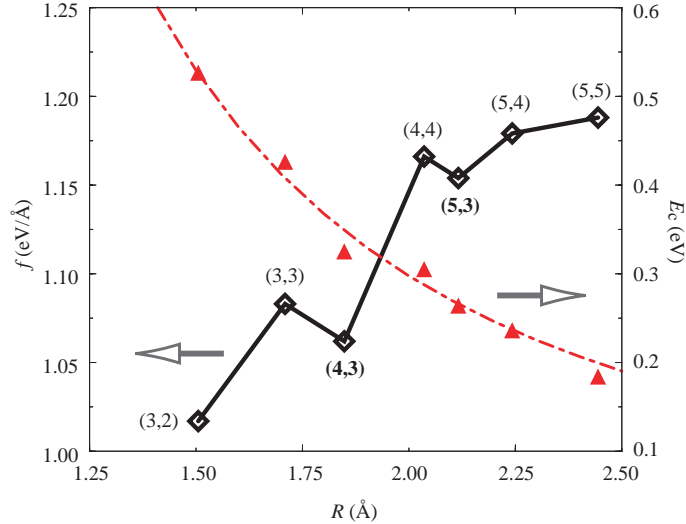


Figure 3. Triangles are calculated curvature energy E_c of free-standing SWNT. Dash-dotted curve is the best fit in the form α/R^2 ($\alpha = 1.19 \text{ eV } \text{\AA}^2$). Diamonds are calculated string tension f of suspended (n, m) gold nanotubes at zero temperature. The local minima of f indicate that $(5, 3)$ and $(4, 3)$ SWNTs are magic.

3. Suspended Tubes

Among three SWNTs with $n = 5$, the $(5, 5)$ tube is energetically the most favorable. This situation is seemingly in disagreement with the experiment indicating that $(5, 3)$ gold tube is the structure observed during the thinning process of gold nanowires [10]. Nevertheless, this apparent contradiction is reconciled by the fact that the calculations are performed for free-standing infinite tubes, whereas the experiment is for a finite tube stretching between two gold electrodes. Hence, E_b should not be taken as a criterion to decide on the long-lived metastable states of suspended nanowires.

Introducing the criterion of minimum string tension rather than the total free energy for the stability of nanowires, Tosatti *et al.* [9] have theoretically investigated a class of gold nanowire structures having a single helical shell covering a central linear strand of atoms. They found that the wire having $(7, 3)$ outer shell exhibits the minimum string tension and was specified as “magic”, in agreement with observation. Here, we carry out string tension analysis for single-wall gold nanotubes without a central strand. The string tension f of a nanowire is defined through the consideration of the positive work done in drawing the wire out of the tips, and is given by [9], $f = F - \mu N/L$. Here, F is free energy of the one unit cell of the wire. At zero temperature, F equals to the total energy E of the wire; μ is the chemical potential of bulk gold, and is calculated to be $\mu \simeq -3.2 \text{ eV}$ within GGA, in consistence with the calculations made for the tubes. Calculated values of the string tension do not exhibit a monotonic decrease as a function of R as displayed in Figure 3. In the plot one immediately recognizes that $(5, 3)$ and $(4, 3)$ SWNTs have lower string tension values as compared to those of their immediate neighboring structures, thus they are favorable magic structures of gold SWNTs. Aside from the reported $(5, 3)$ tube [10], our analysis predicts that the $(4, 3)$ tube with $R = 1.85 \text{ \AA}$ is another candidate for being a “magic” structure which is not observed yet. It appears that the $(5, 3)$ gold SWNT is favored, since it lowers the tension exerted by two gold tips. In principle, the string tension calculation and the geometric relaxation of the structures should be performed self-consistently. The f values reported in Table , however, are results of the first iteration obtained by using the F and L values of the bare unstrained tubes. Nevertheless, we tested that the reduction in f after the full self-consistent calculation is less than 0.3% for the $(5, 3)$ tube, too minor to have any implications on our conclusions.

4. Electronic Structure and Transport

Calculated energy band structures and *ab-initio* ballistic conductance plots of some infinite SWNTs presented in Figure 4 are of particular interest. The tubular character is demonstrated by contour plots of charge density, $\rho_T(\mathbf{r}) = \sum_{i,k}^{occ} \Psi_i^*(\mathbf{r}, k) \Psi_i(\mathbf{r}, k)$. Here $\rho_T(\mathbf{r})$ is dramatically different from that of gold nanowires with a strand at the center. Bands near the Fermi level are derived mainly from the Au-6s orbitals; one band displays significant $5d_{z^2}$ hybridization. Flat $5d$ -bands occur ~ 1 eV below the Fermi level. Despite 1D character of SWNTs, the bands which cross the Fermi level do not allow for Peierls distortion.

A single chain of gold atoms has unit quantum conductance (*i.e.* $G_0 = 2e^2/h$) [11, 12]. It has been usually contemplated that one conductance channel is associated with each helical strand. Accordingly, the ballistic conductance of n -strand gold nanotube would be about nG_0 . The three infinite SWNTs with $n = 5$ have indeed equilibrium conductance values of $5G_0$. However, of the 4-strand nanotubes (4, 4) also has $5G_0$ conductance, while the (4, 3) structure has only three channels for the ballistic conductance. The 3-strand family of nanotubes have $3G_0$ conductance. Since the number of bands crossing the Fermi level determines the conductance of an infinite SWNT, there is no direct correlation between numbers of strands and current transporting channels, rather the cross section of the tube is expected to be crucial in determining the number of channels. Indeed, a minor reduction in the cross section area of the (4, 4) tube due to axial stretching reduces the number of channels from 5 to 3. Dips of size G_0 or $2G_0$ in the conductance plots are another interesting feature one notes. They are due to small gap openings in the energy band diagrams of these helical structures. A recent calculation on the conductance of helical nanowires attributes such characteristic dips to the non-circular cross-section of the wires[17]. Note that the conductance plots of (5, 3) and (4, 3) tubes in Figure 4 have more of those dips since they are more chiral. Finally, we calculated the conductance of finite size (one unit cell) (5, 3) tube which is connected to two fcc gold electrodes through single Au atoms from both ends, and found $G = 1.75G_0$. Dramatic reduction from $5G_0$ (the conductance of infinite tube) is attributed to the contacts with electrodes.

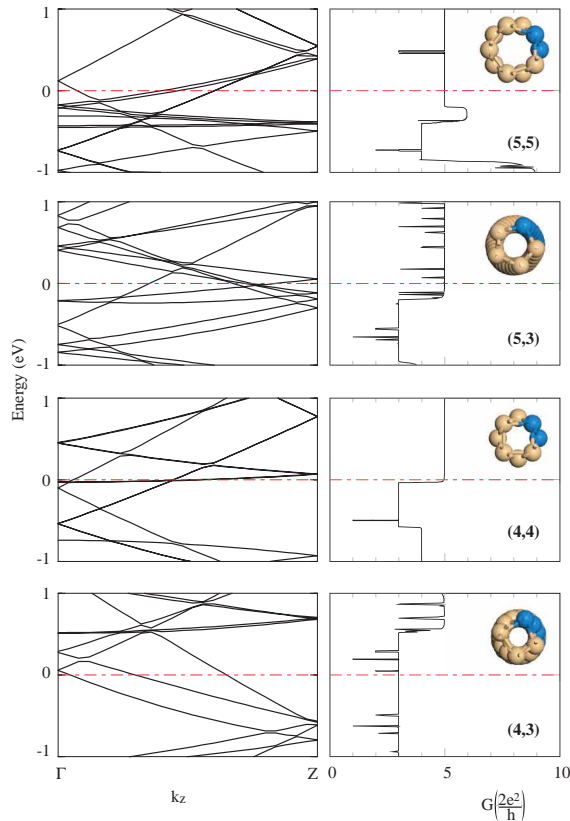


Figure 4. Electronic energy-band structure and ballistic conductance of infinite (5, 5), (5, 3), (4, 4), and (4, 3) gold SWNTs. The Fermi level is set to zero in each panel.

Prediction of chiral currents in chiral (also mechanically stretched) single-wall carbon nanotubes has been of interest because of the self-inductance and nanocoil effects [18]. In principle, chiral current passing through a one-micron (5, 3) SWNT can induce magnetic fields of several Tesla [19]. According to Altshuler-Aronov-Spivak effect [20] electrons circling a cylindrical conductor that encloses a magnetic flux Φ give rise to a periodic oscillating resistance as a function of Φ . The observed short-period oscillations in the magnetoresistance of multi-wall carbon nanotubes have been attributed to chiral currents developed by mechanical stretching of them [21]. It is of interest to reveal whether the electrical current passing through a (5, 3) SWNT has chirality due to the helical structure of the tube. In Figure 5, charge density plots of five states at the Fermi level, corresponding to the conduction channels, clearly indicates the chirality. The geometry of the atomic positions in the (5, 3) tube provides three distinct circumferential directions for the flow of the current. These directions can be defined as AB, AC, and BC in terms of the reference points A, B, C depicted in Figure 4. While the motion along AB and AC directions corresponds to right-handed helices, the helical path along the BC direction is left-handed. The period and direction of chirality are different for different channels; c3 and c4 have opposite chiral directions compared to c1, c2, and c5. Hence, the resultant chirality effect may be weaker than one expects. For the infinite tube, being a transmission eigenchannel of the system, each channel contributes a unit quantum conductance. However, for suspended tubes, the chirality of the net current depends on the combined “nanocoil” effects of the conduction channels, as well as on the contacts.

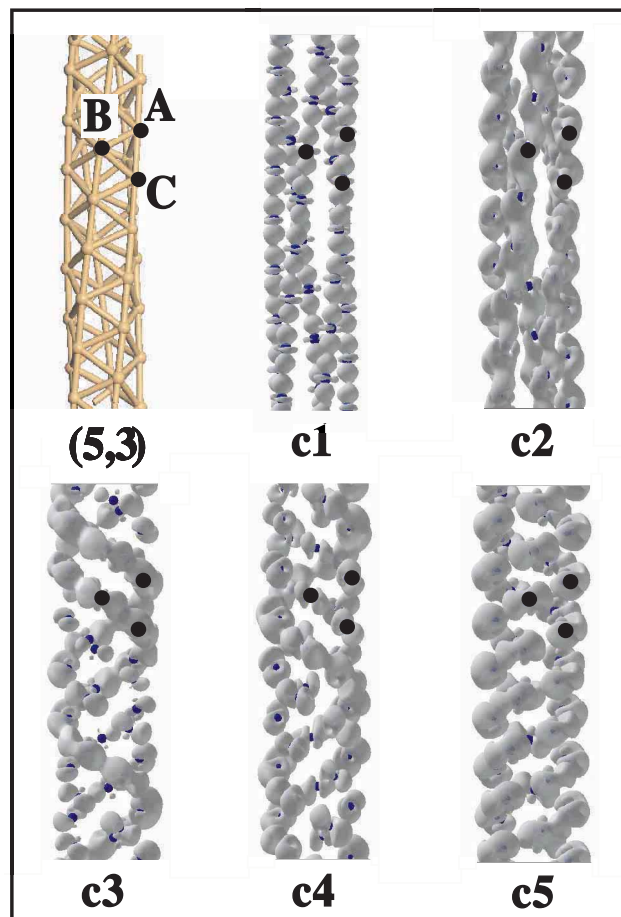


Figure 5. A schematic description of the structure, and isosurfaces for the charge densities of the five states at the Fermi level corresponding to current transporting channels c1, c2, . . . c5. Three reference points A, B, C are shown by dark spots on each plot.

5. Conclusions

In conclusion, we showed that free-standing gold chiral (n, m) tubes with $3 \leq n \leq 5$ are stable and exhibit novel electronic and transport properties. Our analysis explains why the experimentally observed $(5,3)$ tube suspended between two gold tips is favored, and indicates that the string-tension criterion introduced by Tosatti *et al* [9] is also valid for tubular structures. Using this criterion we predict that tip-suspended $(4,3)$ chiral gold tube is another structure that can be observed. We found that there is no direct correlation between the numbers of conduction channels and helical strands making the tubular structure. Current transporting states display different periods and chirality, the combined effects of which lead to weaker chiral currents on SWNTs.

Acknowledgements

Part of the computations for the work described in this paper was supported by TÜBİTAK ULAKBİM High Performance Computing Center.

References

- [1] J. K. Gimzewski and R. Möller, *Phys. Rev. B*, **36**, (1987), 1284.
- [2] S. Ciraci and E. Tekman, *Phys. Rev. B*, **40**, (1989), 11969.
- [3] N. Agraït, J. G. Rodrigo, and S. Vieira, *Phys. Rev. B*, **47**, (1993), 12345; N. Agraït, G. Rubio, and S. Vieira, *Phys. Rev. Lett.*, **74**, (1995), 3995.
- [4] J. I. Pascual, J. Méndez, J. Gómez-Herrero, A. M. Baró, N. García, and V. T. Binh, *Phys. Rev. Lett.*, **71**, (1993), 1852.
- [5] H. Mehrez and S. Ciraci, *Phys. Rev. B*, **56**, (1997), 12632.
- [6] O. Gülseren, F. Ercolessi, and E. Tosatti, *Phys. Rev. Lett.*, **80**, (1998), 3775.
- [7] M. R. Sorensen, M. Brandbyge, and K. W. Jacobsen, *Phys. Rev. B*, **57**, (1998), 3283.
- [8] Y. Kondo and K. Takayanagi, *Science*, **289**, (2000), 606.
- [9] E. Tosatti, S. Prestipino, S. Kostlmeier, A. Dal Corso, and F. D. Di Tolla, *Science*, **291**, (2001), 288.
- [10] Y. Oshima, A. Onga, and K. Takayanagi, *Phys. Rev. Lett.*, **91**, (2003), 205503.
- [11] H. Ohnishi, Y. Kondo, and K. Takayanagi, *Nature (London)*, **395**, (1998), 780.
- [12] A. I. Yanson, G. R. Bollinger, H. E. van den Brom, N. Agraït, and J. M. van Ruitenbeek, *Nature (London)*, **395**, (1998), 783.
- [13] Y. Oshima, H. Koizumi, K. Mouri, H. Hirayama, K. Takayanagi, and Y. Kondo, *Phys. Rev. B*, **65**, (2002), 121401.
- [14] G. Kresse and J. Hafner, *Phys. Rev. B*, **47**, (1993), 558; G. Kresse and J. Furthmüller, *Phys. Rev. B*, **54**, (1996), 11169.
- [15] M. Brandbyge, J.-L. Mozos, P. Ordejón, J. Taylor, and K. Stokbro, *Phys. Rev. B*, **65**, (2002), 165401.
- [16] D. Sánchez-Portal, E. Artacho, J. Junquera, P. Ordejón, A. García, and J. M. Soler, *Phys. Rev. Lett.*, **83**, (1999), 3884.
- [17] M. Okamoto, T. Uda, and K. Takayanagi, *Phys. Rev. B*, **64**, (2001), 033303.
- [18] Y. Miyamoto, A. Rubio, S. G. Louie, and M. L. Cohen, *Phys. Rev. B*, **60**, (1999), 13885.
- [19] V. M. K. Bagci, O. Gülseren, T. Yildirim, Z. Gedik, and S. Ciraci, *Phys. Rev. B*, **66**, (2002), 045409.

- [20] B. L. Altshuler, A. G. Aronov, and B. Z. Spivak, *JETP Lett.*, **33**, (1981), 94.
- [21] A. Bachtold, C. Strunk, J.-P. Salvetat, J.-M. Bonard, L. Forró, T. Nussbaumer, and C. Schönenberger, *Nature (London)*, **397**, (1999) 673.